

Synthesis of Conductive Cu-core / Ag-subshell / polyaniline-shell Nanocomposites and their Antimicrobial Activity

R.M. Mohsen^{1*}, S.M. M.Morsi¹, Y. M. Abu-Ayana¹, A. M. Ghoneim²

¹Department of Polymers & Piments, National Research Centre, 33 El Bohoth St. (Former El Tahrir St.), Dokki, P.O. 12622, Giza, Egypt. Dokki, Cairo

²Microwave Physics and Dielectric Department, National Research Centre, 33 El Bohoth St. (Former El Tahrir St.), Dokki, P.O. 12622, Giza, Egypt. Dokki, Cairo

CORE SHELL technique was used to synthesize conductive Cu-core / Ag-subshell / polyaniline-shell nanocomposites (NCs) and evaluating their antimicrobial activities. This was achieved through two stages, firstly different Cu/Ag core shell nanoparticles (Cu/Ag NPs) were prepared (C/A1, C/A3, C/A5), using electroless plating technique by reduction of AgNO₃ in alcoholic dispersion of Cu NPs at three different weight ratios of AgNO₃: Cu. Secondly, the prepared Cu/Ag NPs were further coated with polyaniline (PANI) by oxidative polymerization of aniline in their aqueous dispersions to form PANI/(Cu/Ag) NCs (NC1, NC3, NC5). XRD patterns of Cu/Ag NPs revealed their bimetallic crystalline structure. SEM micrographs and EDAX data proved formation of Ag thin shell on the surface of Cu core. The concentration of this silvery layer increased from ≈ 38% (C/A1) to 68% (C/A5). SEM and EDAX data of NCs, showed that PANI film wrapped 60% to 63% of Cu/Ag NPs surface that Cu nearly diminished. The synthesized NCs possessed good electrical conductivity that increased with Ag content from 0.52 S/m (NC1) to 13 (NC5) S/m. Good antimicrobial activities (antibacterial and antifungal), of Cu/Ag NPs and their NCs were obtained. Such good conductivity and antimicrobial activity nominate the NCs to be applied in electronic and biotechnical fields.

Keywords: Cu/Ag core shell nanoparticles, Polyaniline nanocomposites, Electrical conductivity, Antimicrobial activity.

Introduction

The use of nanoparticles (NPs) in different areas of life has recently spread, leading to increased research interest in these materials. Amongst these materials are metallic NPs, which occupied an important position for their wide range of application fields, especially in electronics and biotechnology, due to their superior physical and chemical properties [1-3]. Conductive polymer-metal nanocomposites (NCs) occupy superior position among nanostructure materials, due to their different application in electronic and biotechnology fields such as sensors [4,5], biosensors [6-8], corrosion protective coatings [9,10], supercapacitors [11], and electromagnetic shielding devices [12]. They are mainly synthesized from polymer matrix through which metallic fillers are dispersed. Particles size (PS), concentration of matrix, fillers and their bond interactions, are some of many factors greatly

affecting NCs properties [3]. PANI is considered the most promising conductive polymer due to its easy synthesis from cheap monomer, high electrical conductivity, and good stability [4,13]. The conductivity can be controlled by both doping process and type of dopant [14].

The most important metallic NPs are noble metals such as Au, Ag and Pt [15]. The main difficulty in using non-noble metals such as Co, Ni, Fe and Cu arises from their tendency towards oxidation at ambient conditions, particularly as their size gets smaller. Generally, Ag NPs is the most superior metal in conductivity and antimicrobial activity followed by copper [3,16] but Cu is sometimes preferable taking into consideration cost factor. Commonly, metallic NPs are prepared by chemical reduction [16-20] and electrochemical method [21], though various other techniques are involved including laser ablation [22], microwave irradiation [23],

*Corresponding author e-mail: rajiamohsen@yahoo.com

DOI: 10.21608/ejchem.2018.3969.1347

©2017 National Information and Documentation Centre (NIDOC)

biosynthesis [24], sonochemical technique [25], and solvothermal colloidal method [26]. In fact each technique has the advantage and disadvantage, thus choosing the most appropriate method depends on the desired properties and specific applications. Other metallic nanostructures as bimetallic NPs such as, metal nanoalloys [27-30] and core/shell NPs [16,31-33] are of massive importance for their wide range of applications. The properties of bimetallic NAs and core / shell NPs differ from their single constituent metals [34]. Generally, Ag-Cu nanoalloys possess excellent antibacterial and antiseptic characteristics [28-29] by destroying many types of bacteria, viruses and fungi that make them suitable for application in medicine and drug delivery fields [30]. Also, due to their superior electrical conductivity, they are used as sensors, corrosion resistance and composite fillers [27]. Commonly bimetallic nanoalloys can be prepared using chemical reduction and electrochemical method. However, electrochemical is considered the most practical and commercial method to make nanoalloys. Electrochemical method is mainly used for plating metal with more precious metal film. As Cu is susceptible to oxidation on exposure to outer atmosphere, it may be protected by coating with Ag nanolayer [3,16]. This technique is superior to chemical reduction methods, involving strong reducing agents and organic stabilizers, as the particle size (PS) and shape of the NPs, can be controlled by varying the applied current density. Metals commonly employed for platings are silver, copper and nickel. Electroless plating is used for preparing bimetallic NPs by the deposition of metallic thin layer on the other without using electric current [3]. It can be expressed as core shell technique. Bimetallic Cu/Ag core / shell NPs occupy the most important position in such class of nanostructure materials mainly due to their tremendous conductive properties for conductive and decorative inks applications [16,31,32]. Several other studies for preparation Cu / Ag NPs have been carried out, using electrodeposition thermal evaporation techniques under ultrahigh vacuum [32]. Excellent antibacterial and antiseptic characteristic of Cu/Ag NPs nominates them in medical field application [33]. It is worthy to mention that as we discussed above the superior properties of coating the Cu/Ag NPs by conductive polymer, it will also protect Cu from oxidation [32,35]. In this article, synthesis of Cu-core / Ag-subshell / PANI-shell NCs has carried out by coating

PANI on bimetallic Cu/Ag NPs which have been prepared. Their electrical conductivity and antimicrobial activities were evaluated.

Experimental

Materials

Truncated cubical shape Cu NPs of particle size (PS) 1-10 nm (previously prepared and characterized by the authors) [3]. Silver nitrate AgNO_3 was obtained from Sisco Research Laboratories PVT. Ltd. India. Hydrazine monohydrate $\text{N}_2\text{H}_4 \cdot \text{H}_2\text{O}$ 64-65%, reagent grade 98%, was provided from Sigma-Aldrich. Ethylene glycol was obtained from SDFCL Fine Chemical Ltd.. Methyl alcohol 99% was obtained from Sigma Chemicals. Sodium hydroxide pellets 99% was provided from Laboratory Chemicals, Modern Lab. Potassium persulfate 98% was obtained from Fischer Laboratory Reagent. Hydrochloric acid 35-38% was obtained from Fisher Scientific. Aniline monomer was obtained from Merck and distilled under reduced pressure before use.

Methodology

Preparation of bimetallic Cu/Ag core shell NPs

Bimetallic Cu/Ag NPs were prepared by deposition of thin layer of Ag NPs on prepared Cu NPs, using electroless plating technique. In a typical process, 1 g Cu NPs was dispersed in 30 ml methanol by mechanical stirrer using 1 g ethylene glycol as stabilizing agent. Desired amount of AgNO_3 (1g,3g or 5g) was added to the reaction mixture and reduced by 10 g hydrazine monohydrate at pH 8-9 to prepare C/A1, C/A3 and C/A5, respectively. The prepared Cu/Ag NPs was filtered, washed by double distilled water and dried at room temperature.

Synthesis of conductive Cu-core / Ag-subshell / PANI-shell NCs (PANI/(Cu/Ag) NCs

PANI/(Cu/Ag) NCs was synthesized by oxidative polymerization of aniline in the presence of aqueous dispersed Cu/Ag NPs. Typically, 3.75 ml aniline was dissolved in 100 ml distilled water in which 1.5 g C/A NPs was dispersed using 1.5 g ethylene glycol as stabilizing agent. 3g MHCl (doping agent) was added to the reaction mixture with continuous stirring using mechanical stirrer, followed by addition of 1.9 g potassium persulfate dissolved in 100 ml distilled water. Dark greenish precipitate of PANI/(Cu/Ag) NC was obtained, filtered, washed with double distilled water and dried at room temperature. PANI/(Cu/Ag) NCs synthesized from C/A1, C/A3 and C/A5 were

symbolized as NC1, NC3 and NC5, respectively.

Instrumental analysis

XRD analysis

X-ray power diffraction (XRD) patterns were recorded at room temperature using Philips PW 1390 Diffractometer using Ni-filter and CuK radiation source ($\lambda = 1.54 \text{ \AA}$), Japan and operated at 40 kV and 40 mA in the 2θ range $5\text{--}80^\circ$ at the scan speed of 0.05° per second.

The average crystalline size D of NPs is estimated from Scherrer's equation 1 [27]:

$$D = \frac{K\lambda}{\beta \cos \theta} \dots\dots\dots(1)$$

where K is a shape factor constant equals to 0.9, λ is the wave length of X-ray radiation 1.54 \AA , θ is the Bragg diffraction angle and β is the angular line width at half of the maximum intensity (FWHM). The lattice strain ϵ is calculated from equation 2 [36]:

$$\epsilon = \frac{\beta}{4 \tan \theta} \dots\dots\dots(2)$$

FTIR spectroscopy

Fourier transform infrared (FTIR) spectra of sample/KBr pellets were recorded by JASCO FTIR 6100 in the range of $4000\text{--}400 \text{ cm}^{-1}$.

Transmission electron microscopy analysis (TEM)

TEM micrographs were analyzed using High Resolution Transmission Electron Microscope JEOL-2100 TEM, USA.

Scanning electron microscope (SEM)

SEM photos were obtained by Quantum Field Emission Gun 250 SEM instrument with energy-dispersive X-ray spectroscopy (EDAX) system.

Electrical conductivity measurements

AC electrical conductivity was measured in S/m by Hioki 3522-50 LCR Hi Tester (Japan).

Antimicrobial activity measurements

Antibacterial and antifungus activities toward (*Escherichia coli* G⁻ and *Staphylococcus aureus* G⁺) and (*Asprigillus flavus* and *Candida albicans*) were determined using modified Kirby- Bauer disc diffusion [37,38]. Measurements were carried out at "Micro Analytical Center", Faculty of Science – Cairo University.

Results and Discussion

The synthetic steps used to prepare Cu/Ag

NPs and PANI/(Cu/Ag) NC were presented in the schematic diagram displayed in Fig. 1.

Characterization of (Cu/Ag NPs)

XRD of Cu/Ag NPs

Figure 2 shows the XRD diffractograms of the prepared bimetallic Cu/Ag NPs (C/A1, C/A3, C/A5). The emergence of Ag and Cu remarkable peaks in XRD patterns pointed out crystalline formation of both metals. Clear and strong narrow diffraction peaks were obtained indicating high degree of crystallinity. The characteristic peaks of Ag emerged at diffraction angles $2\theta = 38.05\text{--}38.17^\circ$ (111), $44.33\text{--}44.66^\circ$ (200), $64\text{--}64.57^\circ$ (220), $77\text{--}78.33^\circ$ (311), and those related to Cu appeared at $2\theta = 43.28\text{--}43.38^\circ$ (111), $50.17\text{--}50.5^\circ$ (200), 74° (220). They are well agreed with JCPDS standards of Ag NPs (No. 04–0783) and Cu NPs (No. 04–0836). The intensity of Ag diffraction peaks increased with increasing Ag content in Cu/Ag NPs and vice versa with Cu peaks which decreased with increasing Ag content. Table 1 shows the crystallite diameter (D) and lattice strain (L.S.) of Ag and Cu NPs in the Cu/Ag NPs. It shows that D of Ag increased from 11.2 nm in C/A1 to 34.46 nm in C/A5 while for Cu it decreased from 18.89 nm in C/A1 to 14.11 nm in C/A5. The lattice strain which arises due to crystal imperfection and distortion slightly decreased from C/A1 to C/A5.

TEM of Cu / Ag NPs

Figure 3 shows TEM images of C/A5 NPs. It reveals nearly rounded nanocrystals with diameter ranged from 10 nm to 30 nm. Some corner-edged nanocrystals are included in the images.

SEM micrographs and EDAX analysis of Cu/Ag NPs

Figure 4 shows SEM micrographs and EDAX analysis of the synthesized Cu/Ag NPs. EDAX data are given in Table 2. SEM image of C/A1 NPs reveals small spherical flocculates of Ag NPs capping Cu NPs. This silvery coat predominates in SEM photo of C/A5 NPs to appear covering the majority of Cu NPs. The EDAX profiles Cu atoms. The strong and medium signal energy peaks appeared at 2-4 KeV is related to spherical-shaped Ag NPs [39]. The characteristic strongest optical absorption peak of Ag NPs appeared at 3 KeV is due to surface Plasmon resonance [40]. Additionally, three peaks characteristic for Cu NPs are also observed at $\sim 0.85 \text{ KeV}$ representative to L-shell electron and at $\sim 8 \text{ KeV}$ and 8.9 KeV emitted from K-shell electron. EDAX data are

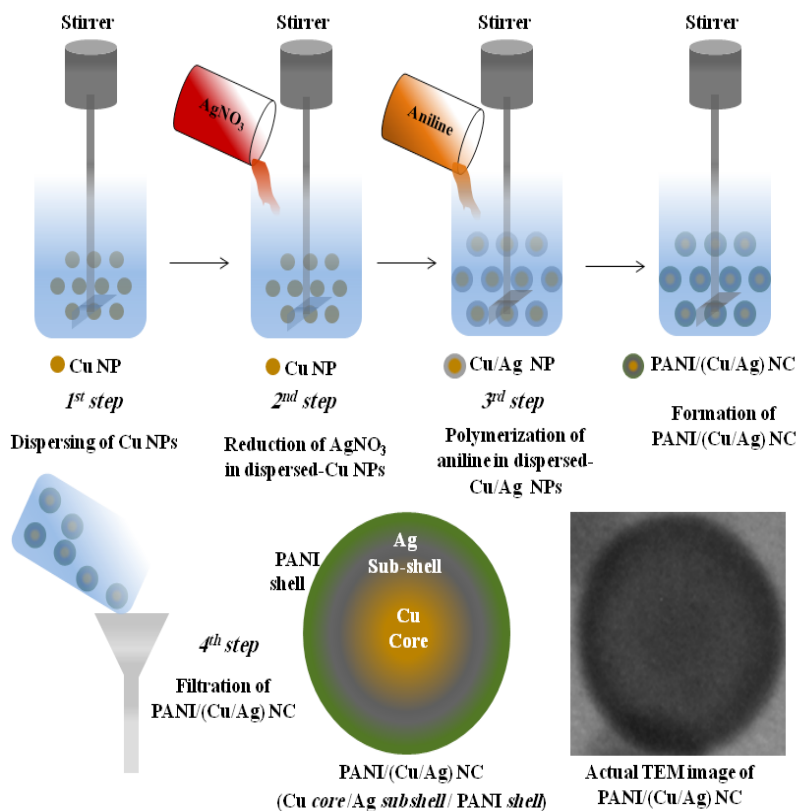


Fig. 1. Schematic diagram of the synthetic pathway used to prepare Cu/Ag NPs and PANI/(Cu/Ag) NC.

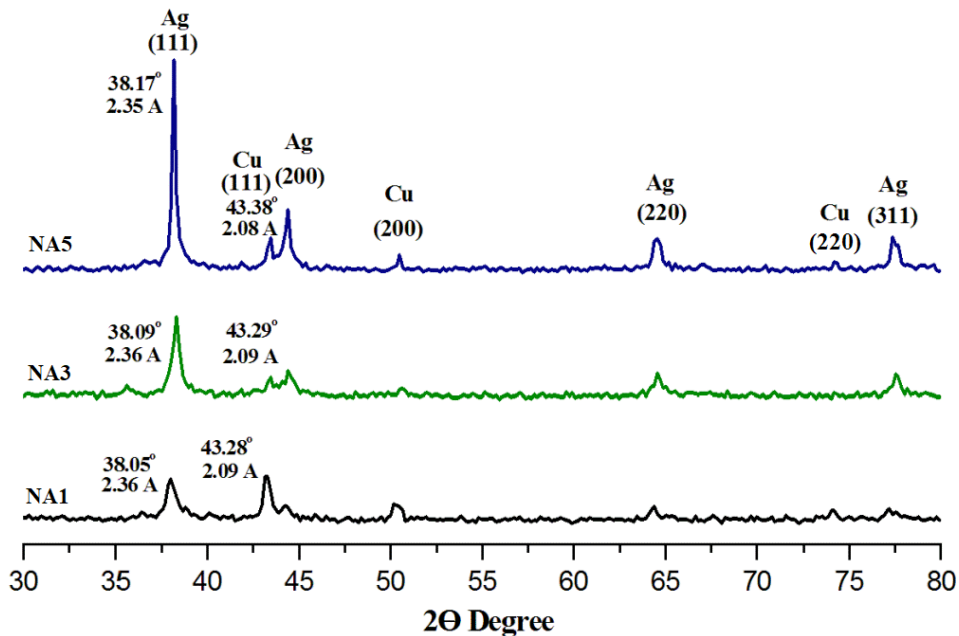


Fig. 2. XRD of Cu /Ag NPs.

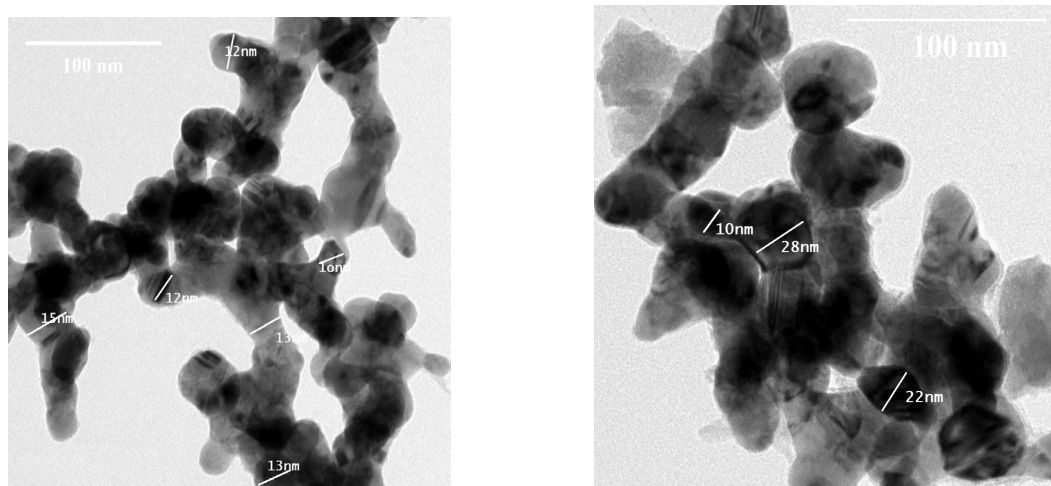


Fig. 3. TEM images of C/A5 NPs.

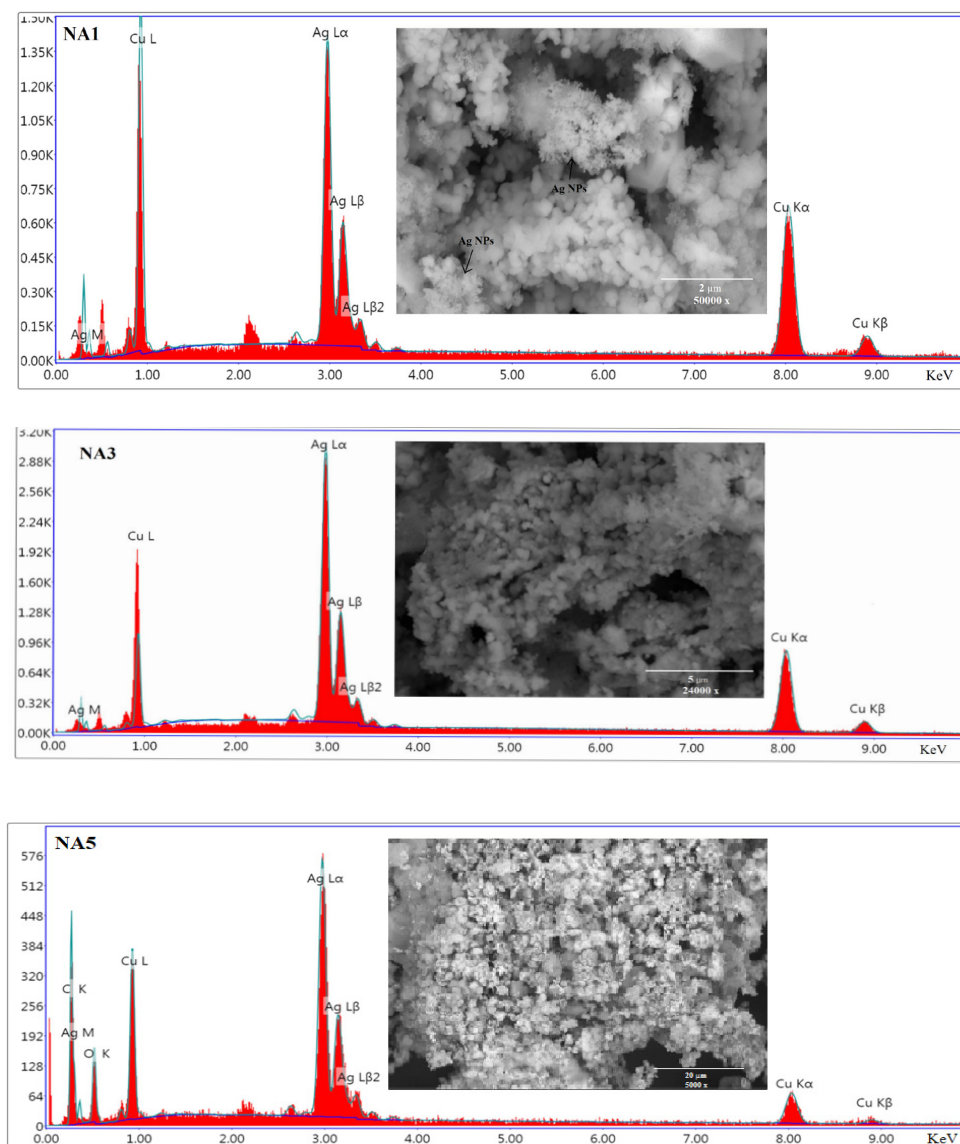


Fig. 4. SEM micrographs and EDAX analysis of Cu/Ag NPs.

TABLE 1. Crystallite diameter (D) and latic strain (L.S.) of in Cu/Ag NPs.

Pea	Ag (111)			Cu (111)		
	C/A1	C/A3	C/A5	C/A1	C/A3	C/A5
D	11.2	14.96	34.46	18.89	15.65	14.11
L.S.	0.0099	0.0074	0.0032	0.0052	0.0063	0.0069

TABLE 2. EDAX data of prepared Cu/Ag NPs.

Reactants ratio AgNO ₃ :Cu	EDAX of Cu/Ag NPs				
	Cu/Ag NPs	Ag:Cu wt. ratio on the surface	wt. %		
			Ag	Cu	
1:1	C/A1	0.615	38.1	61.9	
3:1	C/A3	0.996	49.9	50.1	
5:1	C/A5	2.195	68.7	31.3	

summarized in Table 2 show that as AgNO₃ to Cu ratio increased from 1:1 to 5:1, Ag % increased from 38.1 to 68.7 while Cu % decreased from 61.9 to 31.3.

Characterization of synthesized PANI/(Cu/Ag) NCs *FTIR spectra of the synthesized PANI/(Cu/Ag) NCs*

The FTIR spectra of the synthesized PANI/(Cu/Ag) NCs, (NC1, NC2 and NC5) are given in Fig.5. Since NCs are composed of PANI, Ag NPs and Cu NPs, therefore, PANI characteristic bands are the only one represented in the figure. 3406 cm⁻¹ band is concerning to N-H stretching. 1562-1568 cm⁻¹ and 1485-1498 cm⁻¹ bands are related to C=C stretchings of quinonoid (N=Q=N) and benzenoid (N-B-N) rings, respectively. 1305 cm⁻¹ and 1225 cm⁻¹ bands are assigned to C-N stretchings of both secondary aromatic amine and polaron lattice, respectively. C-H in-plane and out-of-plane bendings of 1,4 disubstituted aromatic rings appeared at 1130cm⁻¹ and 805cm⁻¹, respectively [4,8].

TEM of PANI/(Cu/Ag) NCs

Figure 6 displays TEM photos of PANI/(Cu/Ag) NC5. The images show clear spherical typical core-shell nanoscaled particles. The particles size ranged from 10 nm to 45 nm with the majority between 20 nm to 30 nm. They consist of Cu

core and bilayered shell of silver middle coat and PANI cover. Some small particulates are clearly observed in the images that may be related to a solo item of Cu core constituent.

SEM micrographs and EDAX analysis data of PANI/(Cu/Ag) NCs

Figure 7 shows SEM micrographs and EDAX analysis of PANI/(Cu/Ag) NCs. It revealed that PANI moderately coated Cu/Ag core shell NPs. Some coagulated particles of Ag NPs are observed on the surface. Table 3 summarizes the EDAX analysis data, it shows that PANI coated most of the Cu present on surface, such that it is almost diminished. Also Ag layer were coated by PANI to some degree. Generally no marked variation in NCs surface composition is noticed, whereby the weight percent of PANI and Ag ranged from (60.3 to 63.6), and (35.8 to 39.0) respectively.

Electrical conductivity

Conductivities of synthesized PANI/(Cu/Ag) NCs, are given in Table 4. They increase from 0.52 S/m (in NC1) to 13 S/m (in NC5). Generally, NC3 and NC5 gave high conductivity. This can be attributed to the increase of the relative Ag content to Cu in synthesized PANI/(Cu/Ag) NCs, as Ag is considered the most conductive metal on earth, due to single valence electron that makes it free to move around with little resistance. Cu also is considered one of the few metals that have this particular character, explaining their high

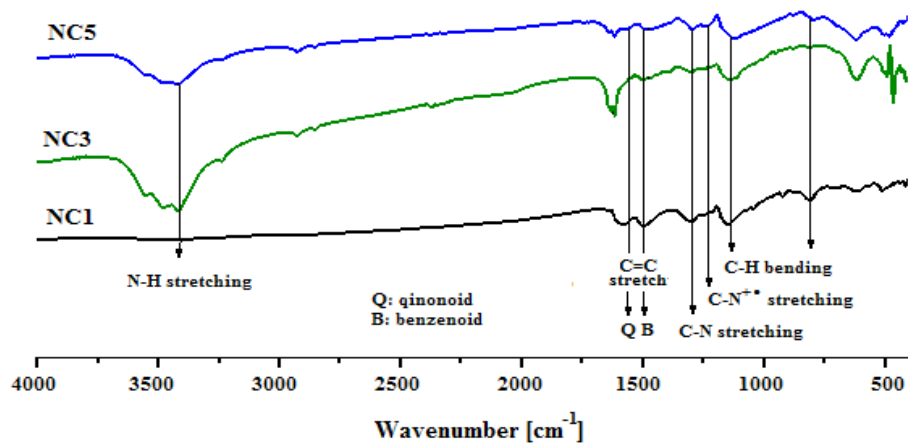


Fig. 5. FTIR spectra of PANI/(Cu/Ag) NCs.

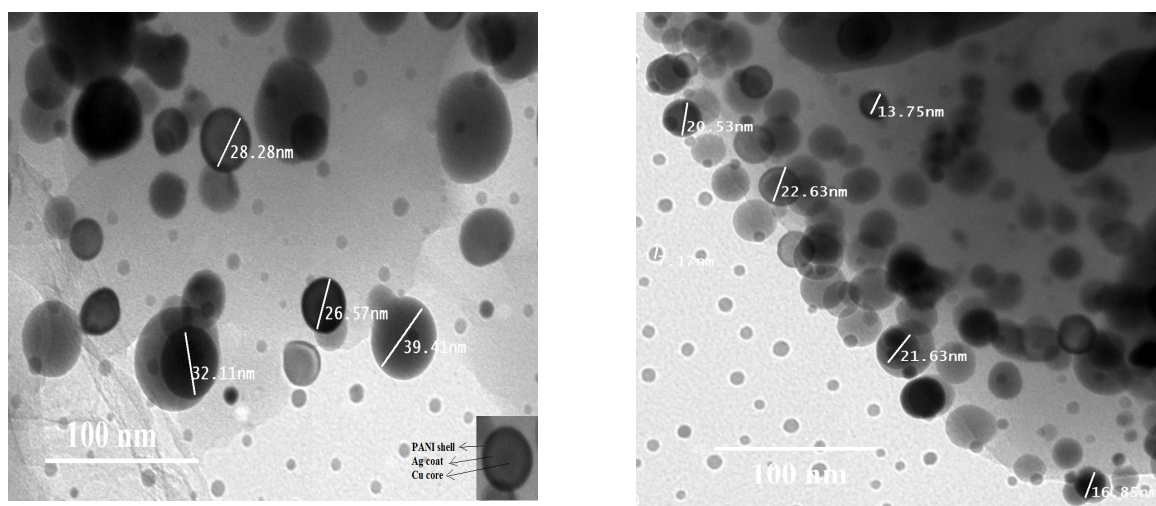


Fig. 6. TEM images of PANI/(Cu/Ag) NC5.

TABLE 3. EDAX data of synthesized PANI/(Cu/Ag) NCs.

Reactants ratio PANI:Cu/Ag NPs	Doped PANI*	EDAX of PANI/(Cu/Ag) NCs					
		NCs	C	N	Cl	Ag%	Cu%
2.55:1	63.6	NC1	33.5	6.2	23.9	35.8	0.6
2.55:1	60.6	NC3	29.6	5.1	25.9	38.9	0.5
2.55:1	60.3	NC5	44.4	10.1	16.8	39.0	0.7

*Approximate estimation of doped PANI from EDAX of C, N and Cl.

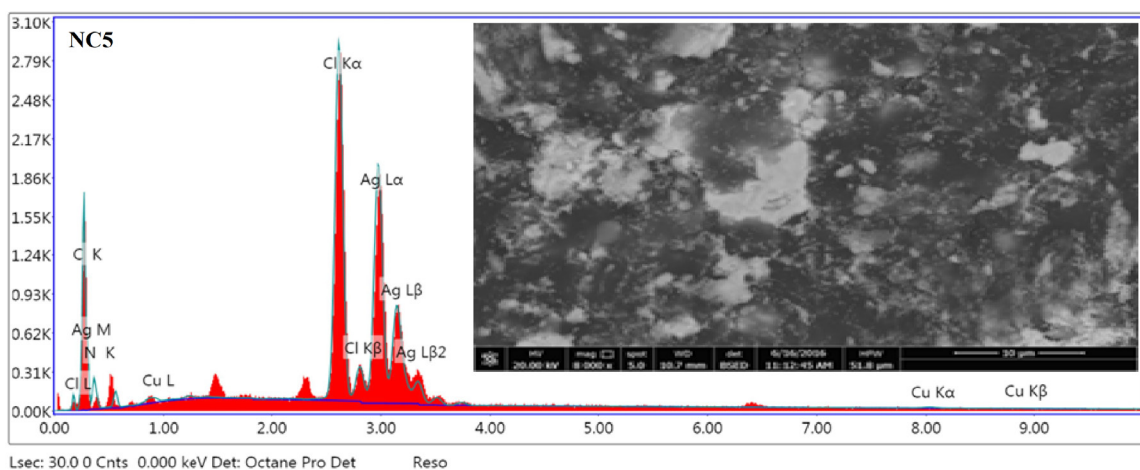
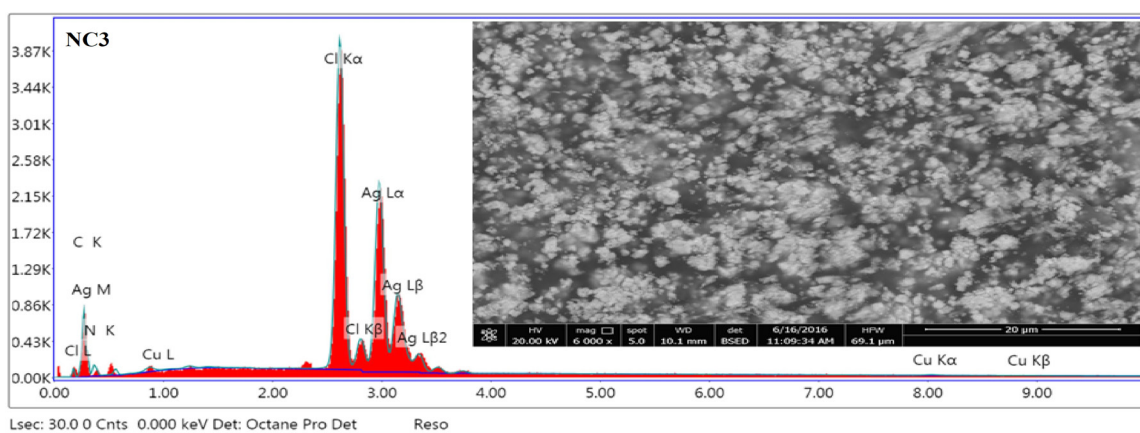
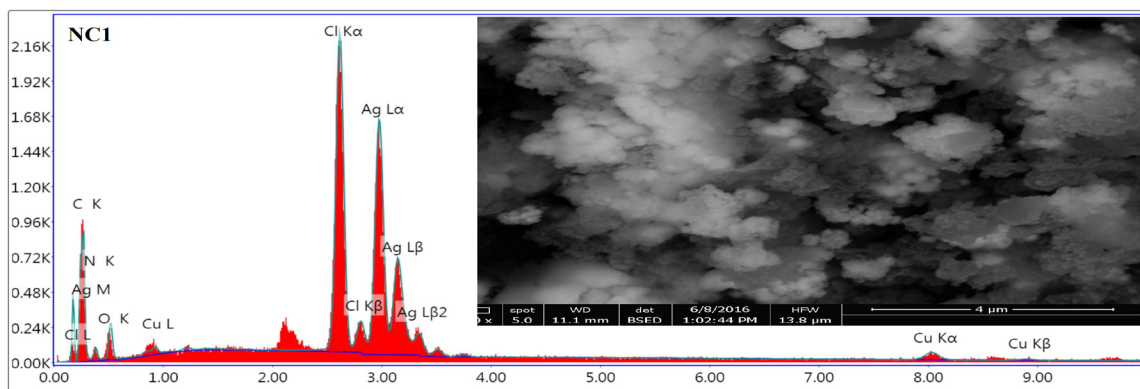


Fig. 7. SEM images and EDAX analysis of PANI/(Cu/Ag) NCs.

TABLE 4. Electrical conductivity of PANI / (Cu/Ag) NCs.

NCs	DC σ (S/m)
NC1	0.52
NC3	9.22
NC5	13.00

conductivity. It is worthy to mention that Ag in Cu/Ag bimetallic nanostructure enhances the electrical migration of Cu ions, leading to high conductivity [27]. Also coating the Cu/Ag NPs by PANI protect the Cu from oxidation.

Antimicrobial activities (antibacterial and antifungal activities)

The antimicrobial activities of Cu/Ag NPs, PANI and NCs relative to standards are represented in Table 5 and Fig. 8. Cu/Ag NPs have medium antibacterial activity to Escherichia coli (G-), while high inhibition is observed towards staphylococcus aureus (G+). They also showed high activity to both Aspergillus flavus and Candida albino fungus, respectively. The antimicrobial activity of them stems from the superior activity of their NPs, allowing them to penetrate the cell wall and kill the microbe, also they generate metal ions in presence of oxygen that can reach the bacteria which NPs can not reach [41,42]. Moreover, as Ag NPs has higher antimicrobial activity than Cu NPs, the increase in Ag to Cu ratio from C/A1 to C/A5 contributed to rise the antibacterial activity, which can be explained by the formation of free radicals of Ag that participate in damaging the microbial cell [43]. It is well known that PANI possesses reasonable antimicrobial and antifungus resistance. Results revealed that doped PANI by hydrochloric acid showed medium and high activity to Escherichia coli (G-) and Aspergillus flavus, respectively, with no activity against Staphylococcus aureus (G+) and Candida albicans (fungus). Therefore, in NCs, PANI layer encapsulating Cu/Ag NPs decreased their antimicrobial activity, as PANI controls the release of metal ions by slowing them down, accordingly excess toxicity of the environment is avoided [41]. The NCs showed medium antibacterial activities towards both G- and G+ bacteria, with slight increase from NC1 to NC5,

whereas they showed excellent antifungal activity towards Aspergillus flavus. They exhibited the same inhibition percentages towards Aspergillus flavus as their counterparts Cu/Ag NPs and also as PANI manifested excellent activity. However NCs are inefficient towards Canaida albicans due to the nil activity of PANI layer.

Conclusion

In this article bimetallic Cu/Ag core shell NPs were prepared using electroless plating of Ag NPs on Cu NPs, by reduction of AgNO_3 in dispersion of Cu NPs. Different weight ratios of AgNO_3 to Cu NPs were used (1:1,3:1, and 5:1). PANI/ (Cu/Ag) NCs were synthesized by oxidative polymerization of aniline in dispersion of the prepared core shell NPs. XRD, FTIR, TEM, SEM and EDAX were used for characterization of both Cu/Ag NPs and their corresponding NCs.

XRD data and TEM images of Cu/Ag NPs indicated the formation of spherical nanoparticles (10-30 nm) of crystalline bimetallic structure. SEM micrographs showed that Ag coated moderately Cu NPs, while EDAX data revealed that thin layer of Ag increased from 38.1 (of C/A1) to 68.7 (of C/A5) while Cu decreased from 61.9 to 31.3 weight percent, respectively.

EDAX data of NCs revealed that PANI mostly coated the uncovered Cu NPs, such that its content nearly diminished (≈ 0.5 weight percent). No marked variation of shell surface composition for all synthesized NCs was observed, as PANI and Ag weight percent ranged from (60-63.5) and (35.8 to 39) respectively.

The electrical conductivity of NCs increased from 0.52 S/m (in NC1) to 13 S/m (in NC5) with increasing of Ag content. They can be used as sensors and as protective coating on

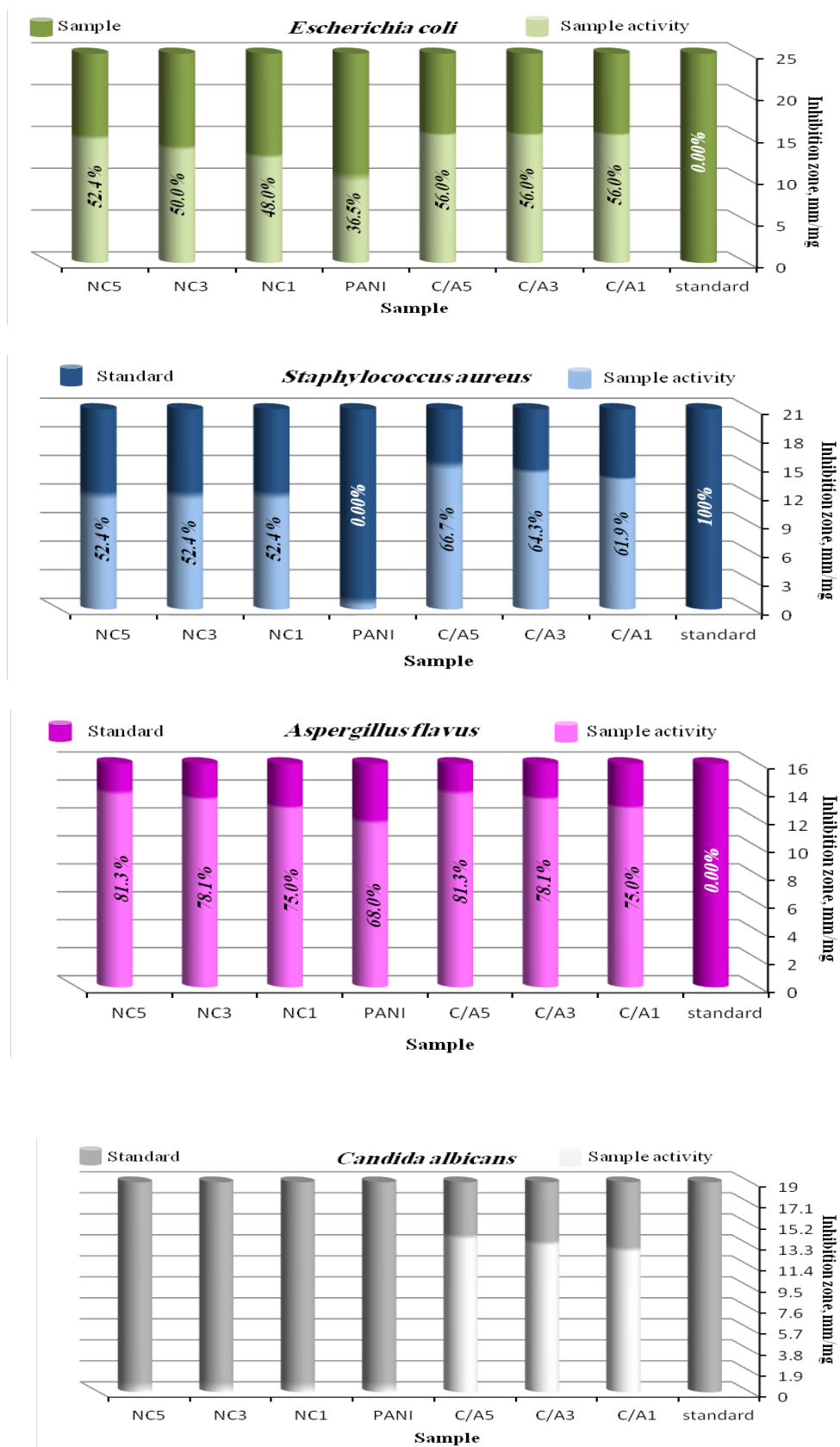


Fig. 8. Antimicrobial and antifungal activities of NPs, NCs and pure PANI and their % in comparison to standards (ampicillin antibacterial agent and amphotericin B antifungal agent).

TABLE 5. Antibacterial and antifungal activity of different prepared Cu/Ag NPs, PANI and synthesized NCs.

Sample	Inhibition zone diameter (mm / mg sample)							
	Escherichia coli (G ⁻)		Staphylococcus aureus (G ⁺)		Aspergillus flavus (Fungus)		Candidaa albicans (Fungus)	
Control : DMSO	0.0		0.0		0.0		0.0	
Standard	Ampicillin antibacterial agent		25		21		--	
	Amphotericin B Antifungal agent		--		--		16	
		% to Standard		% to Standard		% to Standard		% to Standard
C/A1	14	56	13.0	61.9	12.0	75.0	12.0	63.2
C/A3	14	56	13.5	64.3	12.5	78.1	12.5	65.8
C/A5	14	56	14.0	66.7	13.0	81.3	13.0	68.4
PANI pure	9	36	0.0	0.0	11.0	68.8	0.0	0.0
PANI/(C/A1) NC1	12	48	11.0	52.4	12.0	75.0	0.0	0.0
PANI/(C/A3) NC3	12.5	50	11.0	52.4	12.5	78.1	0.0	0.0
PANI/(C/A5) NC5	13	52	11.0	52.4	13.0	81.3	0.0	0.0

Values with respect to standards, 30%, from 30-60% over 60%, and over75% are considered weak, medium, high and excellent respectively.

steel substrate from corrosion. Cu/Ag NPs and their corresponding NCs showed medium-high antibacterial and high antifungal activities, recommending them to be applied as biosensors, detectors and in food packaging field.

Acknowledgment

Great appreciation to National Research Center for the financial support of this research article derived from project No.10050408 (2013-2016). Deep thanks to Prof. Dr. Mohamed Hashem vice president of National Research Center of research affairs and international relations for his continuous support.

References

- Alagarasi A., *Introduction to Nanomaterials*, 1-76 (2011) (available from [http:// www. ncr. \(iitmin /2011\)](http://www.ncr. (iitmin /2011))).
- Nanotechnology, Wikipedia, the free encyclopedia (2014).
- Mohsen R. M., Selim M. M., Aby- Ayana Y. M., Morsi S. M., Ghoneim A. M. and El-Sawy S. M., Nanotechnology and nanomaterials, Chapter 7 in *Nanomaterials & Nanotechnology*, Editor Prof. Waqar Ahmad, Publisher One Central Press (OCP) 145-179 (2016).
- Kunzo P., Polyaniline nanoparticles: Composite for gas sensors preparation and characterization, *Ph.D. Thesis* from STU – FEI, Bratislava (2015).
- Park S. J., Kwon O. S., Lee J. E., Jang J., and Yoon H., Conducting polymer-based nanohybrid transducers: A potential route to high sensitivity and selectively sensors, *Sensors*, **14**, 3604-3630 (2014).
- Mukherjee S., Meshik X., Choi M., Farid S., Datta D., Lan Y., Poduri S., Sarkar K., Baterdene U., En Huang C., Yu Wang Y., Burke P., A graphene and aptamer based liquid gated FET-Like electrochemical biosensor to detect adenosine triphosphate, *Leee Transaction Nanobioscience*, **14** (2015).
- Li J. and Wu N., *Biosensors Based On Nanomaterials and Nanodevices in Nanomaterials and their Applications* book series, Published by CRC Press Taylor Franc Group (2017).
- Abdullah H., Naim N. M., Azmy N. A., and Hamid A. A., PANI-Ag-Cu nanocomposite thin films based impedimetric microbial sensor for detection of E. coli bacteria, *J. of Nanomaterials*, **2014**, 1-8 (2014).

9. John S., Joseph A., Jose A. J., and Narayana B., Enhancement of corrosion protection of mild steel by Chitosan/ zinc oxide nanoparticle composite membrane, *Progress in Organic Coating*, **84**, 28-34 (2015).
10. Tsirimpis A., Kartsonakis I., Danillidis I., Liatasi P., Kordas G., Synthesis of conductive polymeric composite coatings for corrosion protection applications, *Progress in Organic Coatings*, **67**, 389-397 (2010).
11. Giri S., Ghosh D., and Das C.K., In situ synthesis of cobalt doped polyaniline modified graphene composites for high performance supercapacitor electrode materials, *Journal of Electroanalytical Chemistry*, **697**, 32-45 (2013).
12. Pande S., Singh B.P., Mathur R.B., Dhama TL., Saini P., Dhawan S.K., Improved of electromagnetic interference shielding properties of MWCNT- PMMA Composites using layered structures, *Nanoscale Research Letters Journal*, **4**, 327-334 (2009).
13. Chandra S., Kunmar A., Tomar P. K., Synthesis and characterization of copper nanoparticles using reducing agent, *Journal Saudi Chemical Society*, **18**, 149-153 (2014).
14. Das T. K., Prusty S., Review on conducting polymers and their applications, *Polymer Plastics Technology and Engineering*, **51**, 1487-1500 (2012).
15. Ebrahimi G., Rezaei F., Neshati J., Effect of HCl-doped polyaniline nanoparticles on the corrosion protection properties of epoxy coating, *Home*, **36**, 1674-1681 (2015).
16. Grouchko M., Kamyshny M., Magdassi S., Formation of air copper-silver-stable core-shell nanoparticles for inkjet printing, *J. Mater. Chem.*, **19**, 3057-3062 (2009).
17. Mansouri S., Ghader S., Experimental study on effect of different parameters on size and shape of triangular silver nanoparticles prepared by a simple and rapid method in aqueous solution, *Arabian Journal of Chemistry*, **2** 47-53 (2009).
18. Merza K. S., Al-Attabi H. D., Abbas Z. M., Yuser H. A., Comparative study on methods for preparation of gold nanoparticles, *Green on Sustainable Chemistry*, **2**, 20-28 (2012).
19. Sui N., Li X., Liu M., Xiao H., Jiang Y., Zhao J., Yu W. W., Nobel metals nanoparticles synthesized by chemical reduction; under graduate Experiments *Egypt. J. Chem.* **61**, No. 5 (2018)
- for nanomaterials, *Journal of Laboratory Chemical Education*, **2**, 28-32 (2014).
20. Johanna F., Production of Co, Ni, and Cu nanoparticles by hydrogen reduction. *Thesis for the degree Ph.D* of doctor of science in Technology to be presented with due permission for public examination and debate in auditorium F239a at Aalto University School of Science and Technology (Espoo, Finland), on the 27th of August, (2013).
21. Khaydarov R. A., Khaydarov R. R., Gapurova O., Estrin Y., Scheper T., Electrochemical method for the synthesis of silver nanoparticles, *J. Nanoparticles Research*, **11**, 1193-1200 (2009).
22. Mafune F., Kohno J.-Ya, Takeda Y., and Kondow T., Structure and stability of silver nanoparticles in aqueous solution produced by laser ablation, *Journal of phys. Chem. B*, **104**, 8333-8337 (2000).
23. Jagashetty A., Havanoor V., Basavaraja S., Balaji S. D. and Venkataraman A., Microwave assisted route for synthesis of nanosized metal oxides, *Science Technology of Advanced Materials*, **8**, 484-493 (2007).
24. Kulkarni N. and Muddapur U., Biosynthesis of metal nanoparticles: A review, *Journal of Nanotechnology*, 2014 (2014).
25. Kumar B., Smita K., Cumbal L., Debut A., and Pathak R. N., Sonochemical synthesis of silver nanoparticles using starch, *Bioinorganic Chemistry and Applications*, 2014 (2014).
26. Gasaymeh S. S., Radiman S., Heng L.Y., Saion E. and Saeed G.H. M., Synthesis and characterization of silver/polyvinylpyrrolidone (Ag/PVP) nanoparticles using gamma irradiation technique, *J. of Applied Sciences*, **7**, 892-901 (2010).
27. Salam A. A., Singaravelan R., Vasanthi P., Alwar S. B., Electrochemical fabrication of Ag-Cu nanoalloy and its characterization: An investigation, *J. of Nanostructure in Chemistry*, **5**, 383-392 (2015).
28. Valodkar M., Modi S., Pal A., Thakore S., Synthesis and antibacterial activity of Cu, Ag and Cu-Ag alloy nanoparticles: a green approach, *Mat. Res. Bull.* **46**, 384-389 (2011).
29. Taner M., Sayar N., Yulug I. G., Suzer S., Synthesis, characterization and antibacterial investigation of silver-copper nanoalloys, *J. Mater. Chem.*, **21**, 13150-13154 (2011).

30. Bernard V., Zobac O., Sopousek J., Mornstein V., AgCu bimetallic nanoparticles under effect of low intensity ultrasound: the cell viability study in vitro. *J. Cancer Res.* (2014). doi:10.1155/2014/97176.
31. Li Y., Lu Y., Chou K., Liu F., Synthesis and characterization of silver–copper colloidal ink and its performance against electrical migration. *Mat. Res. Bull.* **45**, 1837–1843 (2010).
32. Magdassi S., Grouchko M. and Kamyshny A., Copper nanoparticles for printed electronics: Routes towards achieving oxidation stability, *Materials*, **3**, 4626-4638 (2010).
33. Rousse C., Josse J., Mancier V., Levi S., Gangloff S. C., and Fricoteaux P., Synthesis of copper–silver bimetallic nanopowders for a biomedical approach; study of their antibacterial properties, *RSC Advances*, **6**, 50933-50940 (2016).
34. Paszkiewicz M., Gołębiewska A., Rajski L., Kowal E., Sajdak A., and Medynska A. Z., Synthesis and characterization of monometallic (Ag,Cu) and bimetallic Ag-Cu particles for antimicrobial and antifungal applications, *J. of Nanomaterials*, **2016**, 1-11 (2016).
35. Cioffi N., Ditaranto N., Torsi L., Picca R. A., Giglio E. De, Sabbatini L., Novello G. L., Zacheo T. B., Zambonin P. G., Cioffi N., Synthesis, analytical characterization and bioactivity of Ag and Cu nanoparticles embedded in poly-vinyl-methyl-ketone films, *Analytical and Bioanalytical Chemistry*, **382**, 1912–1918 (2005).
36. Hall W. H., Strain lattice equation, *Acta Metall.* **1**, 22-31 (1953).
37. Bauer A., Kirby W., Sherris C., Turck M., Antibiotic susceptibility testing by a standardized single disk method, *American J. of Clinical Pathology*. **45**, 493-496 (1966).
38. Leibowitz L. D., Ashbee H. R., Evans E. G. V., Chong Y., Mallatova N., Zaidi M., Gibbs D., and Global, A two year global evaluation of the susceptibility of Candida species to fluconazole by disk diffusion, *Diagnostic Microbiology Infect. Disease*, **40**, 27-33 (2001).
39. Arunachalam K.D., Annamalai S.K., Hari S., One step green synthesis and characterization of Leaf extract mediated, biocompatible silver and gold nanoparticles from a memecylon umbellatum, *Nanomedicine*, **8**, 1307-1315 (2013).
40. Kelmani R. C., Ashajyothi C., Oli A. K., Potential bactericidal effect of silver nanoparticles synthesised from enterococcus species, *Oriental Journal of Chemistry*, **30**, 1253-1262 (2014).
41. Potera C., Understanding the germicidal effects of silver nanoparticles, *Forum*, **120** (2012).
42. Raffi M., Mehrwan S., Bhatti T. M., Akhter J. I., Hameed A., Yawar W., Hasan M. M., Investigations into the antibacterial behavior of copper nanoparticles specificity in antimicrobial activity of silver and copper nanoparticles, *Annals of Microbiology*, **60**, 75-80 (2010).
43. Dakal T.C., Kumar A., Majumdar R.S., and Yadav V., Mechanistic Basis of Antimicrobial Actions of Silver Nanoparticles, *Front Microbiol*, **7**, 1831 (2016).

(Received 28/5/2018;
accepted 18/7/2018)

تخليق متراكبات نانومترية موصلة – نواة من النحاس / أغلفة فرعية من الفضة / ذات قشرة بولي أنيليه ونشاطها المضاد للميكروبات

راجيه محمود محسن^١, سمير مرسي محمد مرسي^١, يسريه مصطفى ابو عيانه^١, أحمد محمود غنيم^٢

^١قسم البلمرات والمخضبات - المركز القومي للبحوث - شارع التحرير - الدقي - القاهرة - مصر.

^٢قسم الموجات الميكرونييه والعازلات الكهربيه - المركز القومي للبحوث - شارع التحرير - الدقي - القاهرة - مصر.

تشتهر المعادن بكل من قوة التوصيل الكهربى ومقاومة الميكروبات ويحتل معدن الفضة المكانة الأولى يليه النحاس . ومن الناحية الاقتصادية يفضل النحاس الا أنه من عيوبه قابليته للأكسدة عند التعرض للجو الخارجى. لذا فالسائد طلائه بطبقة رقيقة من الفضة لحمايته باستخدام الطلاء الكهرباء وهو من أكثر الطرق شيوعا . وحيث ان انتاج المواد فى الحجم النانومتري

اجتذب اهميه قصوى فى العالم لخواصها المتميزة التى تفوقت عنها فى الحجم العادى للتطبيقات المختلفه فى شتى المجالات .

يهدف هذا البحث الى تحضير وتقييم متراكبات بوليمريه نانومتريه موصله وذات مقاومه للميكروبات. ويمكن تقسيم العمل بهذا البحث الى قسمين:

- القسم الأول تحضير (silver-copper core shell) حيث يتكون من نواة من جزيئات النحاس ذو الحجم النانومتري , تغطى بجزيئات الفضة النانومترية الحجم بالطلاء دون استخدام الكهرباء electroless plating وذلك باختزال ملح نترات الفضة فى معلق للنحاس النانومتري الحجم. وقد تم استخدام نسب مختلفه بالوزن من نترات الفضة الى النحاس.

- القسم الثانى تحضير متراكب بوليمرى موصل من الأنيلين بنسب مختلفه مع المزيج المعدنى النانومتري المحضر والمشار اليه اعلاه core shell (من النواة من النحاس والمغلف بطبقة رقيقة الفضة). وقد تم التحضير ببلمرة مونومر الأنيلين على سطح core shell .

وتم تقييم جميع الخواص لكل من المزيج والمتراكب البوليمرى الموصل بالأشعة السينيه XRD والاشعه تحت الحمراء FTIR. وباستخدام الميكروسكوب الألكترونى النفاذ TEM لتعيين شكل وحجم الجزيئات النانومترية الحجم . وأيضا باستخدام الميكروسكوب الألكترونى الماسح SEM والمزود باشعه سينييه EDAX لدراسة تركيب السطح وتعيين نسب المكونات المختلفه.

وقد اثبتت القياسات ان جزيئات النحاس النانومترية الحجم قد تم تغطيتها بطبقة رقيقة من جزيئات الفضة النانومترية الحجم بنسب مختلفه (تراوحت بين ٣٨,١ الى ٦٨,٧ %). وقد تمثلت core shell المحضر فى شكل بلورات كرويه نانومتريه الحجم تتراوح بين ١٠-٣٠ نانومتر.

وقد تم الحصول على متراكبات بوليمرية موصله نانومترية بتغطية اسطح core shell بالبولى انيلين وقد اوضحت النتائج اختفاء النحاس نهائيا من السطح وبذا يكون قد تمت حمايته من التعرض للأكسدة وقد اتضح ان تركيب اسطح المتراكبات يتكون فقط من البولى انيلين والفضه (حيث تراوحت نسبة البولى انيلين من ٦٠ الى ٦٣,٥ % بينما الفضة تراوحت نسبها من ٣٥,٨ الى ٣٩ %) بما يفيد أن التغير بسيط فى أسطح المتراكبات البوليمريه الموصله النانومترية المحضرة وقد تمثلت شكل المتراكبات المحضرة على هيئة بلورات كرويه نانومتريه الحجم تتراوح تقريبا بين ٢٠-٣٠ نانومتر. المعدنى أى أن المتراكبات البوليمريه المحضرة يمكن اعتبارها نواة من النحاس النانومتري الحجم مغطى بالفضه جزئيا ثم غلاف خارجى من البولى انيلين والفضه.

تم تقييم التوصيل الكهربى للمتراكبات والتى اثبتت نجاحها واختلاف قيمها طبقا للتركيب حيث تراوحت قوة التوصيل الكهربى بين ٠,٥٢ الى ١٣S/m ويمكن تطبيق هذه المتراكبات فى شتى التطبيقات فى مجال الألكترونيات كما تم تقييم المقاومه للميكروبات لكل من core shell المعدنى وللمتراكبات البوليمريه النانومترية الموصله واثبتت نجاحها ويمكن استخدامها ككشافات وحساسات للميكروبات وفى المواد المستخدمه فى التغليف الغذائى .